J. Plasma Physics (1999), *vol.* 61, *part* 2, *pp.* 275–293. Printed in the United Kingdom
© 1999 Cambridge University Press

Nonlinear dynamics of electron bunches in the presence of dissipative effects

C. KRAFFT,[1] A. VOLOKITIN[2] and M. FLÉ[3]

[1]Laboratoire de Physique des Gaz et des Plasmas, Université Paris Sud, Centre National de la Recherche Scientifique, 91405 Orsay Cedex, France

[2]Institute of Terrestrial Magnetism, Ionosphere and Radiowave Propagation, Academy of Sciences, Troitsk, Moscow Region, 142092, Russia

[3]Laboratoire de Recherche en Informatique, Centre de Ressources Informatiques, Université Paris Sud, 91405 Orsay Cedex, France

(Received 13 July 1998)

The transition phase between two nonlinear regimes of electron-beam–wave interaction depending on the amplitude and the nature of the effective dissipation is investigated with the help of numerical simulations. Effective dissipation due to wave escaping to infinity out of the beam–wave interaction region as well as to collisions in the background plasma is considered. If the dissipation is strong enough, the evolution of the electron beam proceeds in a general way, independently of the type of dissipation and of the nature of the considered waves: structures of strongly concentrated electron bunches are formed. These bunches are not trapped in the wave, and decelerate continuously owing to friction on waves: in the presence of dissipation, the usual quasiperiodic exchange of energy between the wave and the trapped particles, which prevents the wave from collapsing, does not occur. Considering beam interaction with a finite number of waves (modulated wave packet), it is shown that, if the dissipation is strong enough, the structure of electron bunches is dynamically stable in a range of times exceeding several characteristic times of their formation.

1. Introduction

Modulated electron beams are powerful tools for space research on the properties of waves in the very-low-frequency (VLF) range, such as whistler waves. Moreover, they are easier to use than large antennas on satellites, and can radiate over their whole length at the modulation frequency like an artificial antenna (Lavergnat et al. 1984; Lundin et al. 1994, 1995). Emission of VLF waves by beams has been observed in several active space experiments with electron-beam injection (Winckler 1980; Lavergnat 1982; Neubert et al. 1986; Farell et al. 1989; Neubert and Banks 1992; Oraievsky et al. 1994; Raitt 1996). Recent results on Cherenkov emission of whistlers produced during the interaction of a modulated electron beam with a magnetized plasma have also been obtained in laboratory experiments (Krafft et al. 1994a,b; Kostrov et al. 1998). However, only the classical case of the nonlinear interaction of electrostatic waves with a modulated beam, with dissipative effects being neglected, has been given much theoretical consideration (O'Neil et al. 1971; Matsiborko et al. 1972; Jungwirth and Krlin 1975; Pivavorov et al. 1995).

https://doi.org/10.1017/S0022377898007442 Published online by Cambridge University Press

The nonlinear interaction of a monoenergetic electron beam with a wave in the presence of strong dissipation differs considerably from the nondissipative case. Numerical simulations (Ivanov et al. 1973; Carr et al. 1974; Kovalenko 1983) have shown that the dissipative effects prevent the periodic exchange of electron beam and wave energies that usually occurs after the first trapping of electrons in the wave potential. Similar effects were investigated recently in theoretical studies of the nonlinear interaction of a thin electron beam with a quasimonochromatic whistler wave (Volokitin et al. 1997; Krafft and Volokitin 1999). In this case, there is effective dissipation of wave energy due to the losses caused by the free escape of waves from the region of their interaction with the beam. Study of the further evolution of the wave–beam system dynamics reveals the formation of electron bunches that are continuously decelerated owing to the effective friction imposed by the strongly dissipated wave. This effect seems to be rather general, and needs additional consideration, including a study of the transition phase from the regime of quasiperiodic oscillations of trapped bunches to the regime of continuously decelerated electron bunches. The dynamical stability of the bunch structure in the presence of a finite wave packet (or, similarly, interacting with several waves) is another problem that has to be considered.

Therefore we show in this paper that similar nonlinear features accompany the beam–wave evolution in different physical situations, considering either the interaction of whistlers with a beam of finite radius, taking account of the dissipation of waves out of the beam volume, or the beam–wave interaction in a collisional plasma including one or several wave harmonics. In each case, the particle dynamics exhibits the presence of decelerated bunches of trapped particles due to the presence of dissipative effects. In the limit where dissipation vanishes, well-known results have been recovered (see e.g. O'Neil et al. 1971).

Our paper is organized as follows. In Sec. 2, we present the main features of our nonlinear model of beam–whistler-wave interaction, including dissipation due to free escape of waves from the interaction region. In Sec. 3, a general overview of the numerical calculations is given, and the main physical effects are described; characteristics of the transition phase between the dissipative and nondissipative models of beam–wave interaction are studied. Section 4 shows the similarity of physical features accompanying dissipative effects in different situations, by the investigation of beam interaction with one or several waves in a collisional plasma. Section 5 states our conclusions.

2. Nonlinear electron-beam–whistler-wave interaction with wave emission as dissipation

2.1. General description

A theoretical model has been developed (Volokitin et al. 1997; Krafft and Volokitin 1999) in order to study nonlinear whistler-wave emission by a modulated electron beam through the Cherenkov resonance interaction process. Whistler waves are described as quasimonochromatic cylindrical waves slowly varying in space. The case of steady-state beam injection with a fixed modulation frequency is considered; a beam of small radius r_b with cylindrical symmetry is injected along the ambient magnetic field. In this case, the wave evolution is characterized by slow variations of the wave spatial structure along the longitudinal coordinate (distance from the

https://doi.org/10.1017/S0022377898007442 Published online by Cambridge University Press

injector) or, similarly, by slow changes of the wave vector and the wave phase velocity, at a fixed wave frequency.

Wave propagation in the plasma region outside the beam is a linear process that is fully determined by the fields at the beam boundary and by the free propagation of waves to infinity. Thus the corresponding equation of wave amplitude evolution can be readily solved if the wave amplitude at the beam boundary is known. The fields inside the beam region are determined by the beam modulation current as well as by the matching conditions at the beam boundary with the wave fields propagating in the outer plasma region. If the electron beam is narrow (that is, $k_\perp r_b \ll 1$, where $k_\perp$ is the perpendicular wavenumber) then the field structure inside the beam is rather simple, and all fields and potentials can be described in terms of the potential amplitude at the beam centre. With the help of the matching conditions and the free-wave propagation features outside the beam, as well as of the Maxwell equations inside the beam volume, including the beam current as a source term, we have obtained equations describing the slow evolution of the wave amplitude at the centre of the beam according to the slow variation of the beam current modulation. Two physical processes are then pointed out: wave emission by a modulated beam as source term, and loss of wave energy in the beam volume due to wave escape to infinity (effective damping).

The evolution of the beam current modulation is considered self-consistently as the result of nonlinear beam-particle motion in the fields of the resonant whistler wave. In spite of the fact that the radial profile of the beam current can be modified by the action of the whistler, the ambient magnetic field stabilizes the total perpendicular size of the beam, thus allowing us to describe wave fields outside the beam with the approximation of a fixed beam radius. In the description of the beam-electron motion, all nonlinearity is retained, and the only simplification made consists in the drift approximation of the motion in the direction perpendicular to the magnetic field, which is valid in the case of sheared whistlers.

Our approach is analogous in some aspects to the usual description of resonant wave–particle interaction leading to particle trapping. However, our model presents some new and very interesting physical results: owing to the effective damping (escape) of the wave, the behaviour of the resonant particles is different; in our case, there is no quasiperiodic exchange of energy between the wave and the trapped particles. Indeed, in the case where the beam has a finite radius, one has to take into account the irreversible loss of wave momentum and energy due to its escape from the beam–wave interaction volume: the system is not conservative. Thus the energy that the electrons of the beam give to the wave cannot be returned to them, because the main part of this energy is going to infinity: the wave is emitted. Moreover, owing to the loss of momentum by the wave, its wavenumber and phase velocity are decreasing, and the electrons, which remain untrapped after the formation of bunches of trapped particles, cannot be trapped and accelerated by the wave afterwards, because they are not in resonance with it. Owing to a nonlinear shift of the wavenumber, the trapped particles remain in Cherenkov resonance during the deceleration phase.

Note that the numerical solution of the differential system describing the beam–wave nonlinear evolution avoids the use of the more usual PIC simulations (see e.g. Matsumoto and Yasuda 1976; Matsumoto et al. 1980; Omura and Matsumoto 1982; Nishikawa et al. 1994), which need a lot of computer resources to develop clear physical effects.

https://doi.org/10.1017/S0022377898007442 Published online by Cambridge University Press

2.2. The mathematical model

Let us present the framework of our model and the basic assumptions. The whistler wave has a frequency ω that is below the electron gyrofrequency ω_c and well above the lower-hybrid frequency $\omega_{lh} = (\omega_i\omega_c)^{1/2}$, in the case where the electron plasma frequency ω_p exceeds the electron gyrofrequency. We have (in c.g.s. units) $\omega_{c,i} = eB_0/m_{e,i}c$ and $\omega_p^2 = 4\pi ne^2/m_e$; n is the electron density, e is the electron charge, and $m_{e,i}$ are the electron and ion masses. Because the resonant parallel wavenumber k_z (the z axis is directed along the external magnetic field $\mathbf{B}_0$) is much smaller than the perpendicular one ($k_z \ll k_\perp$), the electromagnetic wave fields can be described by the potentials A_z and φ alone, according to

$$\mathbf{B}(B_z, \mathbf{B}_\perp) = \boldsymbol{\nabla} \times \mathbf{A}(A_z, \mathbf{A}_\perp), \quad \mathbf{E}(E_z, \mathbf{E}_\perp) = -\boldsymbol{\nabla}\varphi - \frac{1}{c}\frac{\partial \mathbf{A}}{\partial t}.$$

The perpendicular component $\mathbf{A}_\perp$ of the vector potential is small and can be expressed with the help of A_z.

The corresponding evolution equations for the potentials have been derived from the Maxwell equations in our previous works (Volokitin et al. 1995, 1997). Their solutions are obtained in the form of cylindrical whistler waves produced by the electron beam:

$$\varphi(r,z) = \begin{cases} \displaystyle\sum_{i=1,2} \Theta_i\,(r,z)\, J_1(k_i r_b) H_0^{(i)}(k_i r), & (r > r_b), \\ \displaystyle\sum_{i=1,2} \Theta_i(r,z) H_1^{(i)}\,(k_i r_b)\, J_0(k_i r), & (r < r_b), \end{cases} \tag{2.1}$$

$$A_z(r,z) = \begin{cases} \displaystyle\sum_{i=1,2} \frac{ck_z}{\omega\left(1 + \dfrac{k_i^2c^2}{\omega_p^2}\right)} J_1(k_i r_b) H_0^{(i)}(k_i r) \Theta_i\,(r,z) & (r > r_b), \\ \displaystyle\sum_{i=1,2} \frac{ck_z}{\omega\left(1 + \dfrac{k_i^2c^2}{\omega_p^2}\right)} H_1^{(i)}(k_i r_b) J_0\,(k_i r)\,\Theta_i(r,z) + A_f & (r < r_b), \end{cases} \tag{2.2}$$

with

$$\begin{aligned} A_f &= \frac{4\pi c}{\omega_p^2} j_{bz} \\ &= \frac{2i}{\pi r_b}\frac{ck_z}{\omega}\frac{\Theta_1}{k_1}\frac{\dfrac{k_2^2c^2}{\omega_p^2} - \dfrac{k_1^2c^2}{\omega_p^2}}{\left(1 + \dfrac{k_1^2c^2}{\omega_p^2}\right)\left(1 + \dfrac{k_2^2c^2}{\omega_p^2}\right)}, \end{aligned} \tag{2.3}$$

where $\Theta_i \equiv \Theta_i\,(r_b, z)$ are the cylindrical wave amplitudes; J_n and $H_n^{(i)}$ are respectively the Bessel function of order n and the Hankel function of order n and type i. Here $k_{1,2}$ are the perpendicular wavenumbers, which are solutions of the wave dispersion equation at given ω, and $k_z v_{bz} = \omega$, where v_{bz} is the parallel beam velocity. When, owing to nonlinear processes of resonant beam-particle motion in the whistler wave, the modulation of the longitudinal beam current j_{bz} evolves slowly, that is,

$$j_{bz} = j_{bz}(r,z)\; e^{-i(\omega t - k_z z)} + \text{c.c.}, \tag{2.4a}$$

$$\frac{\partial j_{bz}\,(r,z)}{k_z \partial z} \ll j_{bz}(r,z), \tag{2.4b}$$

https://doi.org/10.1017/S0022377898007442 Published online by Cambridge University Press

the amplitudes $\Theta_i(r,z)$ are slowly varying functions of the coordinate z, i.e. $\partial\Theta_i/k_z\partial z \ll \Theta_i(r,z)$. If the electron beam is narrow (that is, $k_\perp r_b \ll 1$) then the field structure inside the beam is rather simple; all fields and potentials can be described in terms of the potential amplitude at the centre of the beam,

$$\Psi \equiv \varphi(0,z) = \Theta_2 H_1^{(2)}(k_2 r_b) + \Theta_1 H_1^{(1)}(k_1 r_b). \tag{2.5}$$

Boundary conditions allow us to establish the ratio between Θ_1 and Θ_2 as

$$\Theta_1/k_1 = \Theta_2/k_2. \tag{2.6}$$

Then the self-consistent nonlinear evolution of the whistler-wave amplitude along the beam, together with a slow evolution of the electron-beam current modulation, is described by the equation

$$\frac{\partial}{k_z\partial z}\Psi + \kappa\Psi = -i\frac{2\pi\omega}{k_z\omega_p^2} j_{bz}, \tag{2.7}$$

with

$$\kappa = \frac{\widetilde{k}_2^2 - \widetilde{k}_1^2}{\pi(1+\widetilde{k}_1^2)(1+\widetilde{k}_2^2)[x_2 H_1^{(2)}(x_2) + x_1 H_1^{(1)}(x_1)]}, \tag{2.8}$$

where we have used the notation $x_i = k_i r_b$ and $\widetilde{k}_i = ck_i/\omega_p$. With the same accuracy as used to obtain (2.7), the current harmonics on the right-hand side of (2.7) can be averaged on the beam cross-section:

$$\begin{aligned} j_{bz} &\approx \frac{k_z}{2\pi}\int_z^{2\pi/k_z+z} dz\; e^{-ik_z z + i\omega t}\frac{1}{\pi r_b^2}\int_0^{r_b} d^2r\; j_{bz}(z,r,t) \\ &= -en_b v_b \frac{1}{N}\sum_{j=1}^{N} e^{-i\theta_{pj}} \end{aligned} \tag{2.9}$$

where the total number of particles is $N = \pi r_b^2 n_b(2\pi/k_z)$; n_b is the initial beam density and v_b the total beam velocity; $\theta_{pj} = k_z z_j - \omega t$ is the phase of the particle j. Thus the evolution of the wave amplitude Ψ is described by

$$\frac{\partial}{k_z\partial z}\Psi + \kappa\Psi = i\frac{2\pi e n_b v_b^2}{\omega_p^2}\frac{1}{N}\sum_{j=1}^{N} e^{-i\theta_{pj}}. \tag{2.10}$$

This equation has a form that is well known in the theory of wave–beam interaction. However, the term proportional to κ describes new effects of energy loss by wave emission to infinity, and in some sense it is analogous to effective wave damping due to collisions. But, because κ has real and imaginary parts, the analogy is not complete. If the real part of κ represents the rate of emission then the appearance of the imaginary part of κ represents the reversible exchange of wave field energy inside the beam with the outside wave.

The beam-electron motion is considered in a cylindrical coordinate system (r,θ,z) moving with the wave phase velocity $v_{\rm ph} = \omega/k_z$, where the fields are time-independent; $\theta_p = k_z z - \omega t$ is the slowly varying phase describing the longitudinal position z of a particle inside the wave. The electron radial motion in the wave and background magnetic fields is described by the drift approximation, which is valid in the case of sheared whistlers with $\omega \ll \omega_c$. To evaluate the motion of particles in their propagation with the wave, we exclude the time from Newton's equations

https://doi.org/10.1017/S0022377898007442 Published online by Cambridge University Press

with the help of $dz = v_{\rm ph}\,dt$ and get

$$\frac{dr}{dz} = -\frac{eE_\theta}{m_e\omega_c v_{\rm ph}}\left(\frac{v_z - v_{\rm ph}}{v_{\rm ph}}\right), \tag{2.11}$$

$$\frac{d\theta}{dz} = -\frac{e}{rm_e\omega_c v_{\rm ph}}\left(E_r - \frac{v_z}{c}B_\theta\right), \tag{2.12}$$

$$\frac{1}{k_z}\frac{d}{dz}\left(\frac{1}{k_z}\frac{d}{dz}\theta_p\right) = -\frac{e}{\omega v_{\rm ph} m_e}\left(E_z + \frac{B_\theta E_\theta}{B_0} + \frac{B_r E_r}{B_0}\right), \tag{2.13}$$

where the wave fields $\mathbf{E}(E_r, E_\theta, E_z)$ and $\mathbf{B}(B_r, B_\theta, B_z)$ inside the beam have to be expressed as expansions in r/r_b as

$$E_z(r) \approx -ik_z\Psi\left[1 - a_0 + (a_2 - a_1)\left(\frac{r}{2r_b}\right)^2\right]e^{i\theta_p} + \text{c.c.} \tag{2.14a}$$

$$E_r(r) \approx \Psi a_1\left(\frac{r}{2r_b^2}\right)e^{i\theta_p} + \text{c.c.}, \tag{2.14b}$$

$$E_\theta(r) \approx \Psi\frac{i\omega}{c}\frac{\omega_p^2}{c\omega_c}\frac{r}{2}\left(1 - \frac{a_1}{8}\frac{r^2}{r_b^2}\right)e^{i\theta_p} + \text{c.c.}, \tag{2.14c}$$

$$B_z(r) \approx \Psi\frac{\omega_p^2}{c\omega_c}\left(1 - \frac{a_1}{4}\frac{r^2}{r_b^2}\right)e^{i\theta_p} + \text{c.c.}, \tag{2.14d}$$

$$B_r(r) \approx -ik_z\Psi\frac{\omega_p^2 r_b}{c\omega_c}\frac{r}{2r_b}\left(1 - \frac{a_1}{8}\frac{r^2}{r_b^2}\right)e^{i\theta_p} + \text{c.c.}, \tag{2.14e}$$

$$B_\theta(r) \approx \frac{ck_z}{\omega}\Psi a_2\frac{r}{2r_b^2}\,e^{i\theta_p} + \text{c.c.}, \tag{2.14f}$$

with coefficients

$$a_1 = \frac{x_2^3 H_1^{(2)}(x_2) + x_1^3 H_1^{(1)}(x_1)}{x_2 H_1^{(2)}(x_2) + x_1 H_1^{(1)}(x_1)}, \tag{2.15a}$$

$$a_2 = \frac{x_2^3 H_1^{(2)}(x_2)(1 + \widetilde{k}_1^2) + x_1^3 H_1^{(1)}(x_1)(1 + \widetilde{k}_2^2)}{[x_2 H_1^{(2)}(x_2) + x_1 H_1^{(1)}(x_1)](1 + \widetilde{k}_1^2)(1 + \widetilde{k}_2^2)}, \tag{2.15b}$$

$$a_0 = \frac{1}{(1 + \widetilde{k}_1^2)(1 + \widetilde{k}_2^2)}\left[1 + \frac{\widetilde{k}_1^2\left(x_2 H_1^{(2)}(x_2) - \dfrac{2i}{\pi}\right) + \widetilde{k}_2^2\left(x_1 H_1^{(1)}(x_1) + \dfrac{2i}{\pi}\right)}{x_2 H_1^{(2)}(x_2) + x_1 H_1^{(1)}(x_1)}\right]. \tag{2.15c}$$

2.3. Numerical simulation results

The system of equations (2.11)–(2.14) has been solved numerically for parameters typical of active space experiments with artificial beam injection, such as, for example, the recent APEX experiment (Oraievsky et al. 1994). Calculations have been performed with uniform initial particle distributions and a small initial normalized wave amplitude ($y = e\Psi/(\varepsilon^2 m_e v_{\rm ph}^2) \approx 0.1$, where $\varepsilon = (n_b/2n_0)^{1/3}$ and n_0 is the background plasma density). Note that we have tested the numerical properties of our model, in terms of its dependence on the number of macro-electrons representing the beam, on the value of the discrete step used in the numerical approximation of the differential equations, on the initial wave amplitude and on the features of

https://doi.org/10.1017/S0022377898007442 Published online by Cambridge University Press

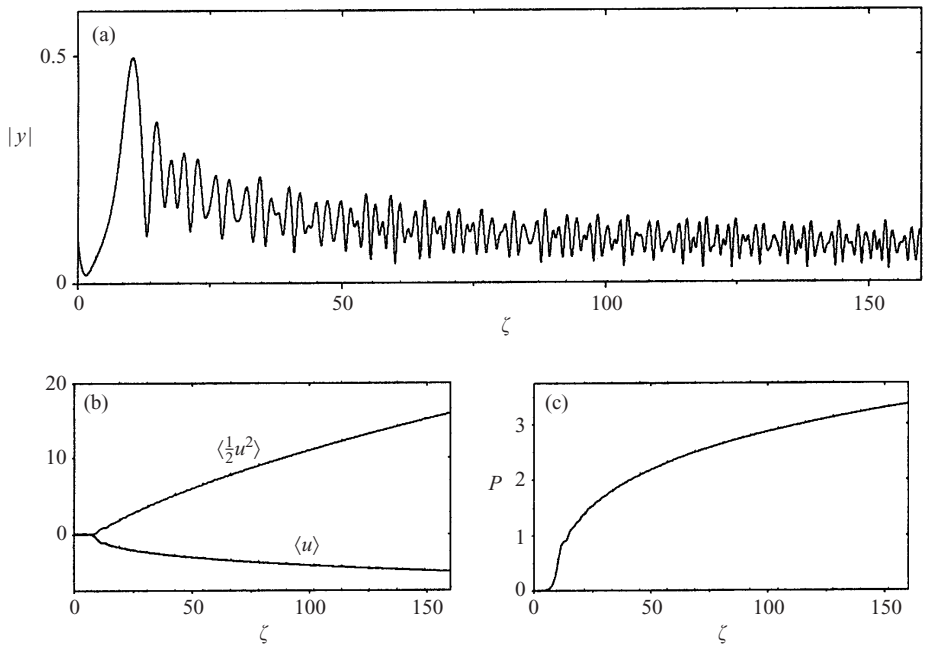


Figure 1. Beam–whistler interaction with dissipation due to wave escape from the beam volume (Re $\kappa \neq 0$). Variation as a function of the normalized longitudinal coordinate ζ of: (a) the normalized wave amplitude $|y|$, where $y = |y|e^{-i\psi_y}$; (b) the total normalized longitudinal beam momentum $p_z \propto \langle u \rangle = \left(\sum_{i=1}^{N}\right)/N$, together with the average normalized square velocity of the particles, $\left\langle \frac{1}{2}u^2 \right\rangle = \left(\sum_{i=1}^{N} u_i^2\right)/2N$; (c) the parameter $P = \int_0^\zeta d\zeta\, |y|^2$, proportional to the emitted wave energy. The parameters are $\omega_p = 3.2 \times 10^7$ Hz, $\omega_c = 9.6 \times 10^6$ Hz ($\omega_p/\omega_c = 3.3$), $\omega = 1.3 \times 10^5$ Hz, $n_b/n_0 = 2.5 \times 10^{-3}$ ($\varepsilon = 0.1077$), Re $\kappa = 0.1436$ ($E_b = 6.3$ keV), $r_b = 3$ m, $v_d = 0.015$, $\Delta v = 0.01$, $N = 6000$. The initial particle distribution is uniform.

the initial distribution of electrons in space and velocity. Calculations have been performed for a number of particles $N = 6000$ and a step $\Delta y = 0.01$, which allow us to obtain numerically independent and physically representative results.

Figures 1 and 2 illustrate the main features of the beam–wave evolution as a function of the normalized distance from the injector $\zeta = \varepsilon k_z z$, in the case of beam–whistler interaction, taking account of dissipation of waves due to their escape from the finite beam volume (the nonlinear model described in Sec. 2.2). Figure 1(a) shows the variation of the normalized wave amplitude $|y| = e|\Psi|/(\varepsilon^2 m_e v_{\rm ph}^2)$, $y = |y|\, e^{-i\psi_y}$, as a function of ζ. Figure 1(b) shows the variation of the total normalized longitudinal beam momentum $p_z \propto \langle u \rangle = \left(\sum_{i=1}^{N} u_i\right)/N$, together with the average normalized square velocity of the particles, $\left\langle \frac{1}{2}u^2 \right\rangle = \left(\sum_{i=1}^{N} u_i^2\right)/2N$, where $u = (k_z v_z/\omega - 1)/\varepsilon$ is the normalized velocity in the wave frame. Figure 1(c) shows the variation of the parameter $P = \int_0^\zeta d\zeta\, |y|^2$, which is proportional to the emitted wave energy. One can see that, after the initial stage where the wave grows according to linear instability until it saturates at $\zeta \approx 10$ owing to particle trapping in the wave potential, there is steady-state behaviour, with wave amplitude oscillations around a decreasing mean level.

https://doi.org/10.1017/S0022377898007442 Published online by Cambridge University Press

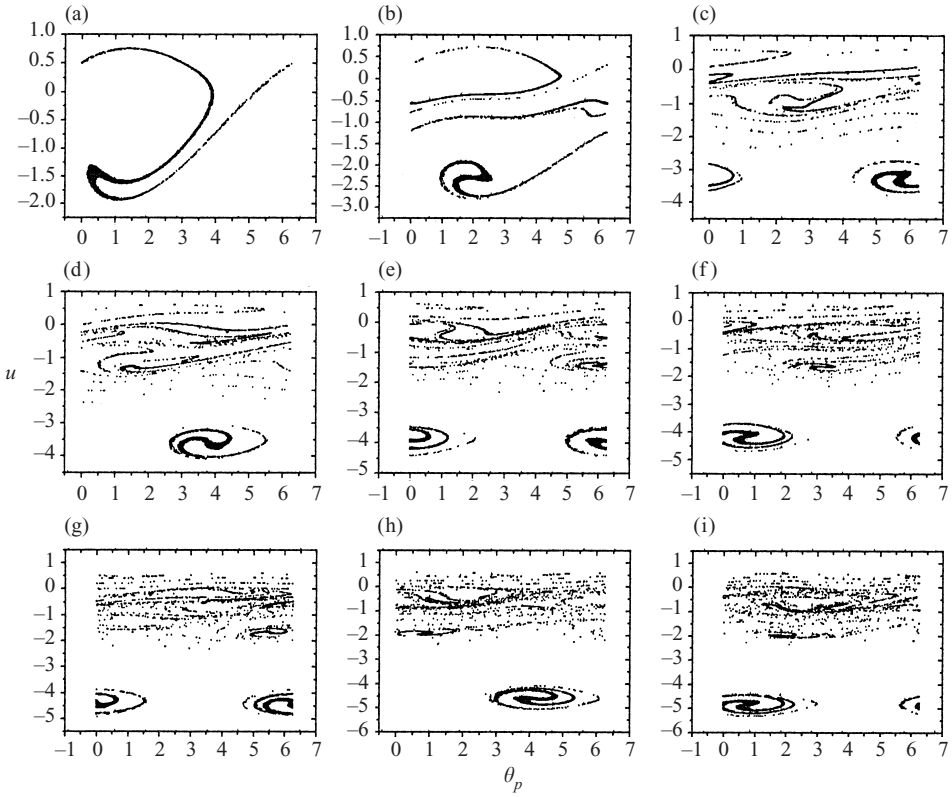


Figure 2. Beam-whistler interaction with dissipation due to wave escape from the beam volume (Re $\kappa \neq 0$). Evolution of the phase space (θ_p, u) at different normalized longitudinal coordinates ζ: (a) $\zeta = 12$; (b) 18; (c) 30; (d) 36; (e) 42; (f) 48; (g) 54; (h) 60; (i) 66. The parameters are the same as in Fig. 1.

The total emitted energy (proportional to $\int_0^\zeta d\zeta\,|y|^2$) and the loss of beam-electron energy (proportional to $\langle u \rangle$) change accordingly (see Figs 1b,c). Since the decrease in the beam electron momentum p_z, which is proportional to $\langle u \rangle$, is mainly due to the deceleration of the trapped particles and the velocity distribution of the passing particles does not change significantly (see also Fig. 2), we may conclude that only the trapped particles are the source of the emission.

Figure 2 shows the evolution of the phase space (θ_p, u) at different distances ζ, exhibiting a clear sequence of particle trapping and the formation of a bunch of decelerated particles, together with untrapped-particle heating. These pictures illustrate some very interesting physical results: owing to the effective escape of the wave, no quasiperiodic exchange of energy between the wave and the trapped particles is observed as is the case when the system is conservative (no dissipation). Since the beam has a finite radius, one has to take into account the irreversible loss of momentum and energy due to wave escape from the beam volume. Thus the energy that the beam electrons give to the wave cannot be returned to them, because the main part of this energy is going to infinity: the wave is emitted. The very close behaviour of wave and current phases (not shown here) indicates that the deceleration of trapped particles is accompanied by a nonlinear wavenumber

https://doi.org/10.1017/S0022377898007442 Published online by Cambridge University Press

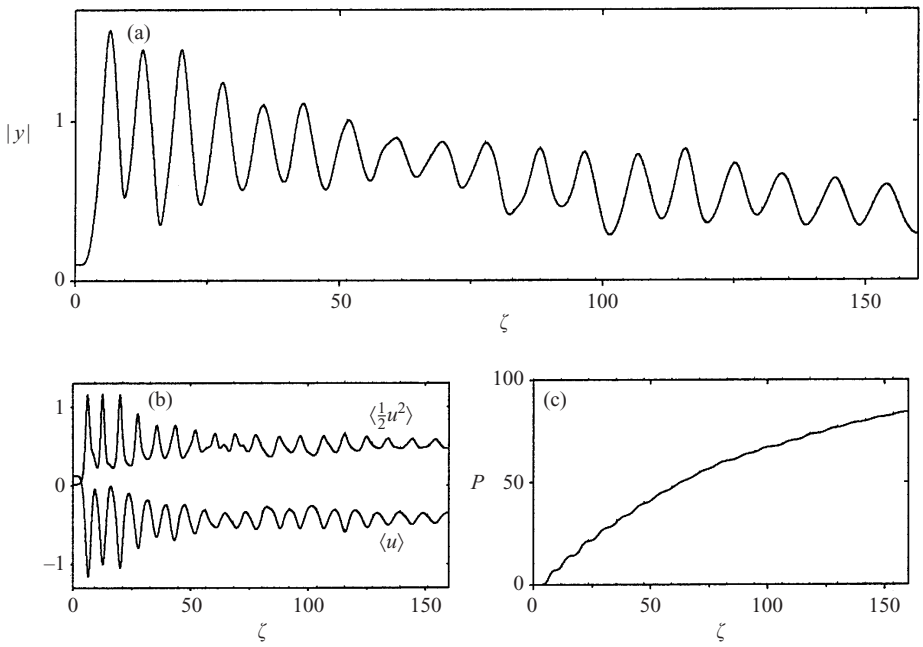


Figure 3. Beam–whistler interaction without dissipation (Re $\kappa \approx 0$). Variation as a function of the normalized longitudinal coordinate ζ of: (a) the normalized wave amplitude $|y|$, where $y = |y|e^{-i\psi_y}$; (b) the total normalized longitudinal beam momentum $p_z \propto \langle u \rangle = \left(\sum_{i=1}^{N} u_i\right)/N$, together with the average normalized square velocity of the particles, $\left\langle \frac{1}{2}u^2 \right\rangle = \left(\sum_{i=1}^{N} u_i^2\right)/2N$; (c) the parameter $P = \int_0^\zeta d\zeta\ |y|^2$, proportional to the emitted wave energy. The parameters are $\omega_p = 3.2 \times 10^7$ Hz, $\omega_c = 9.6 \times 10^6$ Hz ($\omega_p/\omega_c = 3.3$), $\omega = 1.3 \times 10^5$ Hz, $n_b/n_0 = 2.5 \times 10^{-3}$ ($\varepsilon = 0.1077$), Re $\kappa = 0.001$ ($E_b = 6.3148$ keV), $r_b = 3$ m, $v_d = 0.015$, $\Delta v = 0.01$ and $N = 6000$. The initial particle distribution is uniform.

shift Δk_z (Δk_z is proportional to $\partial\psi_y/\partial\zeta$) to conserve Cherenkov resonance between wave and particles.

The bunched electrons are in resonance with the wave, and so they are subjected to much stronger radial motion than the untrapped particles. According to (2.11), the radial drift velocity of these particles keeps its negative sign, and the particles drift to the centre of the beam when ζ grows ($d\rho/d\zeta < 0$, where $\rho = r/r_b$). Although the radial focusing of the bunch is rather slow, it can result, after a long evolution ($\zeta > 300$), in a significant decrease in the bunch radius (more than two times). The radial motion of the untrapped particles is negligible (small oscillations).

Figures 3 and 4 show diagnostics similar to those presented in Figs 1 and 2 respectively, but for a greater value of the beam energy E_b, i.e. for a lower value of Re κ (Re $\kappa \approx 0.001$). Recall that the case Re $\kappa \approx 0$ corresponds to the so-called double-pole case (represented by point G on the index surface of Fig. 5), where the two whistler waves present in the plasma have the same propagation features (their perpendicular wavenumbers satisfy $k_1 \approx k_2$; see also (2.8)) and where the wave group velocity $\mathbf{v}_g$ is directed along the ambient magnetic field: at this point, the wave energy flow remains confined in the beam volume, which consists of a cylinder of radius r_b extending along the ambient magnetic field and the beam velocity directions. Indeed, numerical calculations show that when Re κ tends to

https://doi.org/10.1017/S0022377898007442 Published online by Cambridge University Press

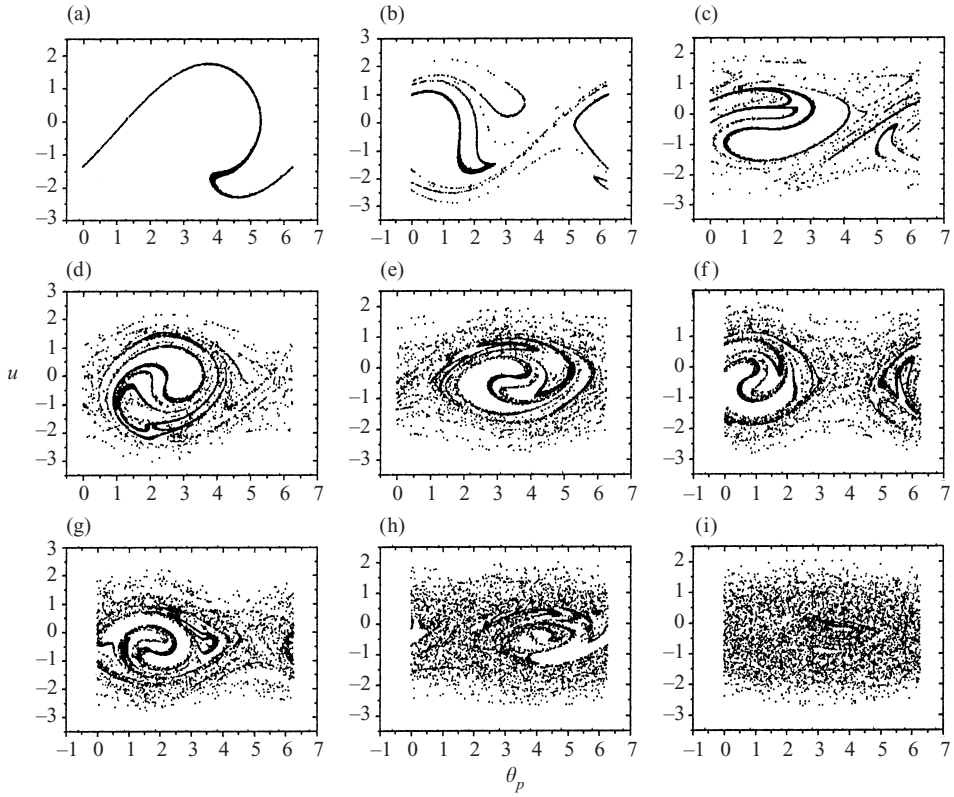


Figure 4. Beam–whistler interaction without dissipation (Re $\kappa \approx 0$). Evolution of the phase space (θ_p, u) at different normalized longitudinal coordinates ζ: (a) $\zeta = 6$; (b) 12; (c) 24; (d) 36; (e) 48; (f) 54; (g) 66; (h) 120; (i) 240. The parameters are the same as in Fig. 3.

zero, effective dissipation no longer occurs: the system becomes similar to the well-known beam–plasma interaction without dissipation. No irreversible exchange of energy from particles to wave occurs, and the system is conservative: no wave is escaping from the beam volume; this kind of beam–wave interaction has been well studied both theoretically (O'Neil et al. 1971) and experimentally (Porkolab and Chang 1978).

On Fig. 3(a), the evolution of the wave amplitude shows that the wave exchanges periodically energy with the particles: its amplitude does not decrease with ζ but exhibits oscillations around a constant mean level, with a period equal to the trapping wavelength; the wave is sustained from collapsing by the particle-trapping process, and the beam electrons are sloshing back and forth in the troughs of the wave. In the phase space, trapped electrons are rotating, and when they reach their minimum velocity, the wave reaches its maximum amplitude; since the system is conservative, the wave damps, while electrons continue their rotation and regain energy; thus the wave amplitude oscillates about a mean value. This behaviour is different from that observed in the case where Re $\kappa \neq 0$ (Fig. 1), where the wave amplitude damps owing to the dissipation of waves emitted from the finite beam volume and going to infinity. Figure 3(b) presents the variation of the beam momentum $p_z \propto \langle u \rangle$ and the average normalized square velocity of the particles, $\langle \frac{1}{2} u^2 \rangle$, which oscillate around a constant mean value, whereas the emitted wave

https://doi.org/10.1017/S0022377898007442 Published online by Cambridge University Press

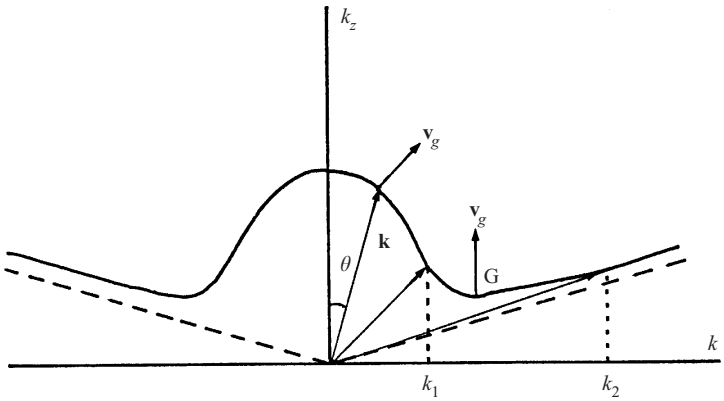


Figure 5. Index surface of whistlers for $\omega < \frac{1}{2}\omega_c$. Variation of the parallel wavenumber k_z as a function of the perpendicular wavenumber k; the point G is the so-called double pole where the two waves with $k = k_1$ and $k = k_2$ are merging; $\mathbf{v}_g$ is the wave group velocity and θ the propagation angle with respect to the ambient magnetic field directed along k_z.

energy $P = \int_0^\zeta d\zeta\ |y|^2$ reaches a saturation level at large ζ (Fig. 3c). Figure 4 shows the corresponding phase-space evolution, where the usual trapping process occurs. At some distance from the injector, the vortex structures disappear through phase mixing (Figs 4h–i), resulting in wave amplitude damping at large ζ (see Fig. 3a). In contrast, when Re $\kappa \neq 0$, decelerated electron bunches already exist at large ζ.

3. Effects of collisional dissipation

3.1. Beam interaction with a single wave

As physical features similar to those occurring for Re $\kappa \neq 0$ (see (2.8) and Sec. 2.3) have been observed in numerical simulations for the case of beam–whistler interaction including collisions (Ivanov et al. 1973; Carr et al. 1974; Kovalenko 1983), it is interesting to compare these results with those obtained with our nonlinear model, where dissipation is due to wave emission from the interaction region and not to electron–ion and electron–neutral collisions. Let us recall the equation of evolution of the electrostatic-wave amplitude in a collisional plasma:

$$\frac{\partial y}{\partial \zeta} + \nu_e\, y = i\frac{1}{N}\sum_{j=1}^{N} e^{-i\theta_{pj}}, \tag{3.1}$$

where ν_e is a real normalized dissipation factor proportional to the ratio of the collision frequency ν_c to the increment γ of the beam instability; $y = |y|e^{-i\psi_y}$ is the normalized complex wave amplitude, N the total number of beam electrons, θ_p the phase of particles and ζ the normalized distance from the beam injector. Neglecting the radial and azimuthal electron motion, the electron dynamics is simply described by

$$\frac{d^2\theta_p}{d\zeta^2} = -e_z = iye^{i\theta_p} + \text{c.c.}, \tag{3.2a}$$

$$\frac{d\theta_p}{d\zeta} = u, \tag{3.2b}$$

https://doi.org/10.1017/S0022377898007442 Published online by Cambridge University Press

where e_z is the normalized longitudinal electric field and u the normalized longitudinal velocity in the wave frame.

For such a simple model, similar physical effects as observed previously in Figs 1 and 2 have been evidenced, as shown by Fig. 6, which presents the wave-amplitude, and the phase-space evolutions for $\nu_e = 1$; the latter show decelerated vortex structures of trapped particles, together with an appreciable fraction of beam particles that remain untrapped. The wave amplitude evolution shows linear growth followed by saturation and oscillations around a mean value.

The asymptotic solution (when ζ is very large) of (3.1) and (3.2) can be obtained as

$$|y| \approx -\frac{n_{\rm tr}}{u} \sin\varphi \tag{3.3}$$

$$\frac{du}{d\zeta} \approx -\frac{n_{\rm tr}}{u} \sin 2\varphi \tag{3.4}$$

$$\frac{du^2}{d\zeta} \approx -2n_{\rm tr} \sin 2\varphi \approx \text{const}, \tag{3.5}$$

where $n_{\rm tr} = N_{\rm tr}/N$ is the ratio of the number $N_{\rm tr}$ of trapped particles to the total number N of particles, and $\varphi = \theta_p + \psi_y + \frac{1}{2}\pi$. We have taken into account here the facts that the current is only due to the trapped particles and that the wave and the bunch of trapped particles remain in phase, i.e.

$$\theta_p + \psi_y = \varphi - \tfrac{1}{2}\pi \approx \text{const}, \quad \text{or} \quad \frac{d\psi_y}{d\zeta} \approx -u. \tag{3.6}$$

The form of the asymptotic solution (3.5) is confirmed by the numerical solution of (3.1) and (3.2), which shows that the bunch of trapped particles remains in phase with the wave and that the beam kinetic energy $\langle \frac{1}{2}u^2 \rangle$ is proportional to ζ.

Numerical simulations confirm that, when ζ is large, $d\langle \frac{1}{2}u^2 \rangle/d\zeta$ tends to a constant, as expected from (3.5). Figure 7 shows the variation of the asymptotic slope $d\langle \frac{1}{2}u^2 \rangle/d\zeta$ and of the fraction $n_{\rm tr}$ of trapped particles as a function of ν_e. When ν_e increases, collisional effects lead to greater wave dissipation and to stronger bunch deceleration; correspondingly, the wave is more effectively damped. The number of trapped particles decreases with increasing ν_e, that is when the collisional frequency becomes large compared with the growth rate of the beam instability.

3.2. Beam interaction with a wave packet

As we have seen above, the velocity of the electron bunches decreases continuously as a function of time (see the phase-space plots in Fig. 6), and thus the bunched particles can start interactions with other waves of smaller phase velocities than the initial wave. This can be the case for a beam interacting with waves in a waveguide, if the discrete spectrum of eigenmodes includes modes with close phase velocities. Let us consider here the example of beam interaction with a packet of Langmuir waves of finite width in k space. Usually one expects that, after first a particle trapping and a transient regime, the wave–beam system evolves to a stage that can be described by the quasilinear theory. However, if the dissipation is strong, it can prevent the stochastic mixing of wave phases required for the validity of quasilinear theory. If so, the phases of all waves in the wave packet become strongly correlated, and the modulated electron beam can be considered as a nonlinear van Kampen mode propagating in the plasma, with strong collisional dissipation of electric field

https://doi.org/10.1017/S0022377898007442 Published online by Cambridge University Press

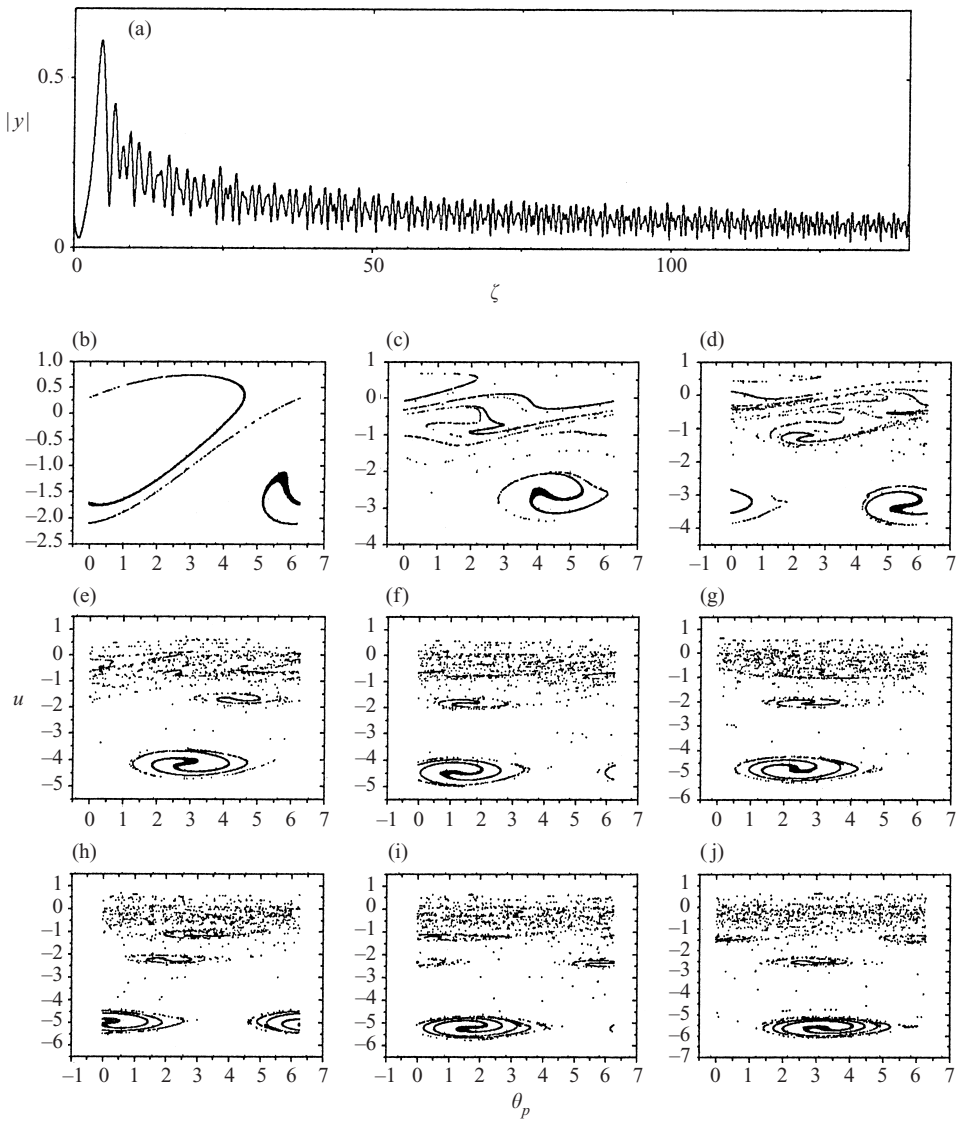


Figure 6. Interaction of a beam with an electrostatic wave in a collisional plasma. (a) Evolution of the wave amplitude $|y|$ as a function of ζ. (b)–(j) Phase-space plots (θ_p, u) at (b) $\zeta = 6$, (c) 12, (d) 18, (e) 30, (f) 36, (g) 42, (h) 48, (i) 54 and (j) 66. The normalized dissipation factor is $\nu_e = 1$ and $N = 6000$; the same initial particle distribution has been used as in previous figures.

oscillations. In this case, the nonsinusoidal electron density variation in the bunches (which can be decomposed into several harmonics) produces forced electric field perturbations in the form of modulated wave packets propagating together with the electron beam.

In order to study this process in a simplified case, let us derive the system of equations describing the beam interaction with several wave harmonics. Starting from the Poisson equation and using the linear hydrodynamic description in a cold

https://doi.org/10.1017/S0022377898007442 Published online by Cambridge University Press

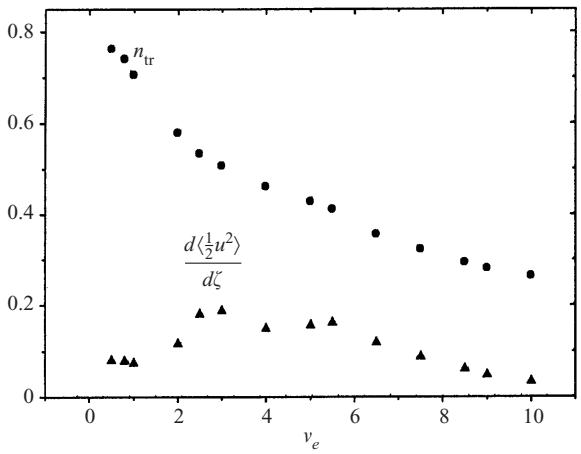


Figure 7. Interaction of a beam with an electrostatic wave in a collisional plasma. Variation, as functions of the normalized collisional factor ν_e, of the slope $d\left\langle \frac{1}{2}u^2 \right\rangle / d\zeta$ of the beam kinetic energy with respect to the normalized distance ζ to the injector (triangles), and of the ratio n_{tr} of the number of trapped particles to the total number of particles (circles). The same initial particle distribution has been used as in previous figures, and $N = 6000$.

plasma for one-dimensional Langmuir waves interacting with the beam, we get

$$\left\{ \frac{d}{dt} - i\left[\omega - \frac{\omega^2(k)}{\omega + i\nu_c} \right] \right\} E'_k = -4\pi j_{bk} e^{i\omega t}$$
$$= (4\pi e n_b v_b) \int dv_0 \int \frac{dz_0}{L} f(v, z, t) \exp[i(\omega t - kz)] \quad (3.7)$$

where $\omega^2(k) = \omega_p^2(1 + 3k^2 r_d^2)$; ν_c is the cold-plasma electron collision frequency, r_d the Debye radius and $f(v, z, t)$ the beam electron distribution; j_{bk} the beam current and E'_k the electric field associated with the wavenumber k. According to Liouville's theorem, we have $\int dv\, dz = \int dv_0\, dz_0$, where $z = z(v_0, z_0, t)$ and $v = v(v_0, z_0, t)$ (where v_0 and z_0 are the initial particles coordinates and velocities).

Writing

$$z = v_b t + \delta z, \quad (3.8)$$

$$\delta\omega_k = \omega - \frac{\omega^2(k)}{\omega}, \qquad \omega = \omega(k_0) = v_b k_0 \quad (3.9)$$

$$k = k_0 + \delta k, \qquad \delta k = \frac{2\pi}{L} m \ll k_0, \qquad m = 0, \pm 1, \ldots, m_*, \quad (3.10)$$

where k_0 is the wavenumber for which the Cherenkov relation (3.9) is satisfied and $M = 2m_* + 1$ is the total number of wave harmonics, we get

$$\left[\frac{d}{dt} + \nu_c - i\,(\delta\omega_k + v_b \delta k) \right] E_k = 4\pi e n_b v_b \int dv_0 \int \frac{dz_0}{L} f(v, z, t) \exp(-ik\delta z)$$
$$= \frac{4\pi e n_b v_b}{N} \sum_{i=1}^{N} e^{-ikz_i}, \quad (3.11)$$

where $E_k = E'_k e^{iv_b \delta k t}$; z_i is the longitudinal particle position in the frame of the

https://doi.org/10.1017/S0022377898007442 Published online by Cambridge University Press

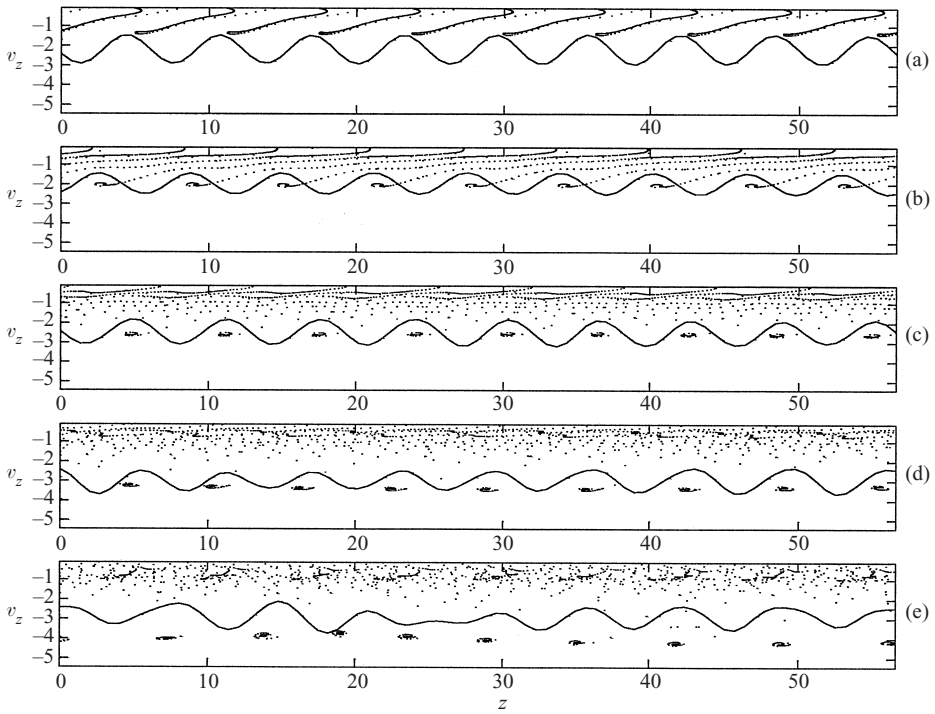


Figure 8. Interaction of a beam with a packet of electrostatic waves in a collisional plasma (case of strong dissipation). Phase space plots (v_z, z) at (a) $\tau = 45$, (b) 70, (c) 90, (d) 120 and (e) 150. The normalized dissipation factor $\nu' = 3.3$ and $N = 2000$. The initial particle distribution is sinusoidally modulated in velocity around a mean value v_b. For a suitable reference on the phase plot, the profiles of the electric field potential are superimposed on the figures (continuous lines, in arbitary units).

resonant wave. The Lorentz equation can be written as

$$\frac{d^2\delta z}{dt^2} \equiv \frac{d}{dt}\delta v_z = \frac{-e}{m_e}\sum_k E'_k \exp(ikz - i\omega t)$$
$$= \frac{-e}{m_e}\sum_k E_k \exp(ik\delta z). \tag{3.12}$$

Using the normalization

$$x = \frac{\omega^2}{\omega_p^2}k_0\delta z, \qquad \tau = \omega t\left(\frac{n_b}{n_0}\right)^{1/3}, \qquad A_k = E_k\frac{ek_0}{m_e\omega_p^2}\left(\frac{n_b}{n_0}\right)^{-2/3} \tag{3.13a}$$

$$\nu' = \frac{\nu_c}{\omega}\left(\frac{n_b}{n_0}\right)^{-1/3}, \qquad \Delta_k = \frac{\delta\omega_k + v_b\delta k}{\omega}\left(\frac{n_b}{n_0}\right)^{-1/3}, \qquad k' = \frac{\omega_p^2}{\omega^2}\frac{k}{k_0}, \tag{3.13b}$$

we obtain the equations describing the beam–wave-packet evolution as

$$\left(\frac{d}{d\tau} + \nu' - i\Delta_k\right)A_k = \frac{1}{N}\sum_{i=1}^{N} e^{-ik'x_i}, \tag{3.14}$$

https://doi.org/10.1017/S0022377898007442 Published online by Cambridge University Press

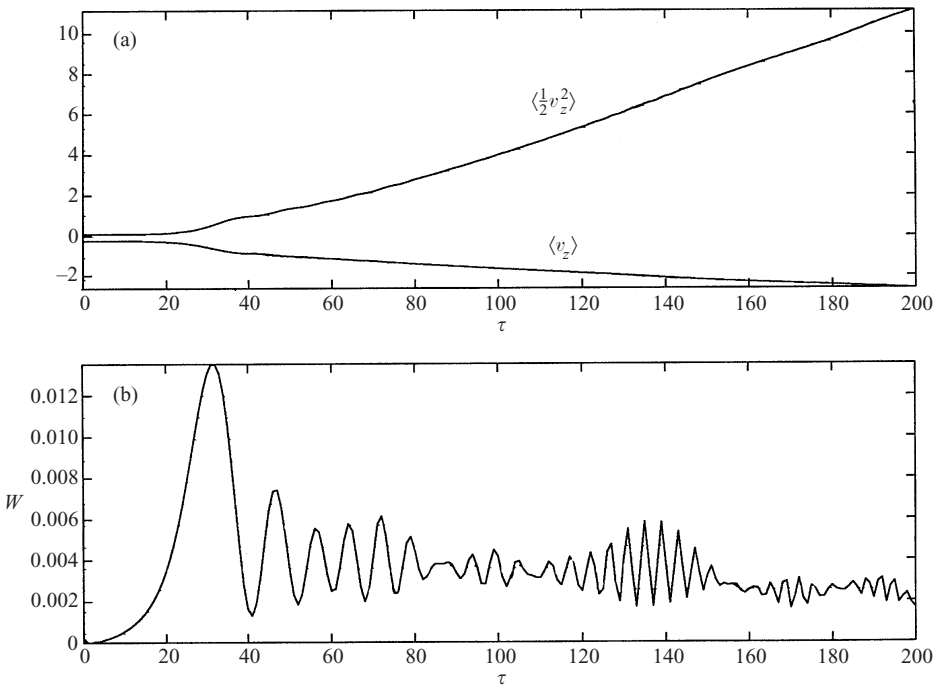


Figure 9. Interaction of a beam with a packet of electrostatic waves in a collisional plasma. Evolution with the normalized time τ of (a) the beam-electron momentum $p_z \propto \langle v_z \rangle$ and the beam kinetic energy $\left\langle \frac{1}{2} v_z^2 \right\rangle$, as well as (b) the total field energy $W = \sum_k |A_k|^2$. The parameters are the same as in Fig. 8.

$$\frac{d^2x}{d\tau^2} = -\sum_{k'} A_k e^{ik'x_i} + \text{c.c.} \tag{3.15}$$

These equations have been solved numerically for different numbers of harmonics m and values of the normalized dissipation ν'. As initial state, we have used cold electron-beam distributions with velocities v_z modulated according to $v_z = v_b + \delta v_b \cos(k_0 z)$ and small random amplitudes of wave harmonics. Below, we present only the main results of the simulations; the details concerning the transition phase from structured bunches to quasilinear regimes will be presented elsewhere.

Numerical simulations show that the formation and dynamics of electron bunches in the case of strong dissipation ($\nu' \geqslant 2$) occur essentially in the same way as in the one-wave-harmonic case (see Sec. 3.1). Figure 8 presents phase plots for five different times τ, together with the variation of the potential amplitude as a function of z (continuous lines on plots, in arbitrary units), for nine wave harmonics and $\nu' = 3.3$; nine vortices can be seen, which are decelerated with roughly the same velocities. The time evolutions of the total field energy $W = \sum_k |A_k|^2$, the beam-electron momentum $p_z \propto \langle v_z \rangle$ and the beam energy $\langle \frac{1}{2} v_z^2 \rangle$ are shown in Fig. 9 for the same parameters. One can see that the evolution of wave and beam physical parameters is similar to what was observed above (Secs 2 and 3.1) and that very clear electron-bunch structures exist up to $\tau \approx 150$. Note that the resonant wave dominates in the wave spectrum only up to $\tau \approx 50$; then the spectrum becomes wide (at

https://doi.org/10.1017/S0022377898007442 Published online by Cambridge University Press

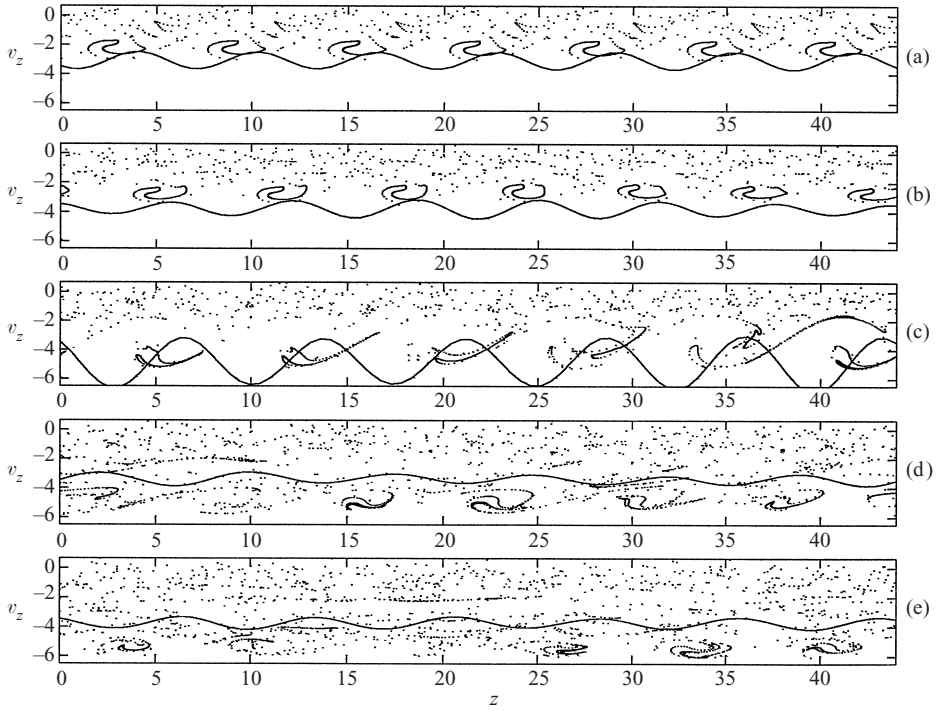


Figure 10. Interaction of a beam with a packet of electrostatic waves in a collisional plasma (case of weak dissipation). Phase space plots (v_z, z) at (a) $\tau = 45$, (b) 70, (c) 90, (d) 120 and (e) 150. The normalized dissipation factor $\nu' = 0.2$ and $N = 2000$. The initial particle distribution is modulated in velocity around a mean value v_b. For a suitable reference on the phase plot, the profiles of electric field potential are superimposed on the figures (continuous lines, in arbitary units).

large times, it can be compared to white noise). In spite of that, the structures of continuously decelerated electron bunches continue to exist, and they only become unstable at later stages of the time evolution. The later dynamics shows that the bunches have a tendency to 'collide': this is due to an instability that leads to bunches with slightly different velocities, and faster bunches can catch up with slower bunches. As a result, they tend to form more complicated structures, as 'superbunches'. At the same time, the electron-beam velocity distribution function shows the typical two-narrow-peak profile (decelerated bunch and heated bulk). The bunched electrons are continuously decelerating with a roughly constant rate of deceleration at all times after the bunch formation (see Fig. 9).

For comparison, Fig. 10 presents phase plots of the beam–wave system for the case of weak dissipation, with $\nu' = 0.2$. The electron bunches are much less clearly formed after $\tau \approx 50$, and their deceleration is very small.

4. Conclusions

We have investigated, with the help of numerical simulations, the transition phase between two nonlinear regimes of electron-beam–quasimonochromatic-wave interaction, depending on the amplitude and the nature of the effective dissipation.

https://doi.org/10.1017/S0022377898007442 Published online by Cambridge University Press

Effective dissipation due to wave escape to infinity from the beam–wave interaction region, as well as to collisions in the background plasma, has been considered. The results show that if the dissipation is strong enough, the evolution of the electron beam proceeds in a general way, independently of the type of dissipation and the nature of the considered waves: structures of strongly concentrated electron bunches are formed. These bunches are not trapped in the wave, and decelerate continuously owing to friction on waves: in the presence of dissipation, the usual quasiperiodic exchange of energy between the wave and the trapped particles, which prevents the wave from collapsing, does not occur. This paper has also presented the first study of bunch dynamics in their interactions with a finite number of waves (modulated wave packet). It has been shown that if the dissipation is strong enough, the structure of bunches is dynamically stable in a range of times exceeding several characteristic times of their formation.

Acknowledgements

The authors acknowledge financial support from the Centre National de la Recherche Scientifique (CNRS, France) and from the Russian Academy of Sciences (RFBR Grant 98-05-65025).

References

Carr, W., Jones, R., Boyd, D., Manickam, J. and Seidl, M. 1974 Saturation of beam–plasma instability in a lossy plasma. *Phys. Fluids* **17**, 1638.

Farell, W. M., Gurnett, D. A. and Goertz, C. K. 1989 Coherent Cherenkov radiation from the Spacelab 2 electron beam. *J. Geophys. Res.* **94**, 443.

Ivanov, A. A., Parail, V. V. and Soboleva, T. K. 1973 Nonlinear theory of the interaction between a monoenergetic beam and a dense plasma. *Soviet Phys. JETP* **36**, 887.

Jungwirth, K. and Krlin, L. 1975 Generation of an intense stationary wave in modulated beam–plasma systems. *Plasma Phys.* **17**, 861.

Kostrov, A., Starodubtsev, M., Krafft, C., Matthieussent, G. and Volokitin, A. 1998 Interaction of a modulated electron beam with a magnetoactive plasma. *JETP Lett.*, **67**, 400.

Kovalenko, V. P. 1983 Electron bunches in nonlinear collective beam–plasma interaction. *Soviet Phys. Usp.* **26**, 116.

Krafft, C. and Volokitin, A. 1999 Nonlinear interaction of whistler waves with a modulated thin electron beam. *Phys. Plasmas* (in press).

Krafft, C., Thévenet, P., Matthieussent, G., Lundin, B., Belmont, G., Lembège, B., Solomon, J., Lavergnat, J. and Lehner, T. 1994a Whistler emission by a modulated electron beam. *Phys. Rev. Lett.* **72**, 649.

Krafft, C., Matthieussent, G., Thévenet, P., and Bresson, S. 1994b Interaction of a density modulated electron beam with a magnetized plasma: emission of whistler waves. *Phys. Plasmas* **1**, 2163.

Lavergnat, J., Dechambre, M., Pellat, R., Kushnerevsky, Yu. V. and Pulinets, S. A. 1980 Waves observed by the ARAKS experiment: generalities. *Ann. Geophys.* **36**, 323.

Lavergnat, J., Lehner, T. and Matthieussent, G. 1984 Coherent spontaneous emission from a modulated beam injected in a magnetized plasma. *Phys. Fluids* **27**, 7.

Lundin, B., Chmyrev, V., Krafft, C. and Matthieussent, G. 1994 VLF emission produced by a rarefied electron beam during active experiments in the Earth ionosphere: conditions of observation of the emission. *J. Geophys. Res.* **99**, 14987.

Lundin, B., Krafft, C. and Matthieussent, G. 1995 Whistler emission produced by modulated electron beams injected into the ionosphere. *J. Geophys. Res.* **100**, 3703.

https://doi.org/10.1017/S0022377898007442 Published online by Cambridge University Press

Matsiborko, N. G., Onishchenko, I. N., Shapiro, V. D. and Shevchenko, V. I. 1972 Of nonlinear theory of instability of a mono-energetic electron beam in plasma. *Plasma Phys.* **14**, 1204.

Matsumoto, H. and Yasuda, Y. 1976 Computer simulation of nonlinear interaction between a monochromatic whistler wave and an electron beam. *Phys. Fluids* **19**, 1513.

Matsumoto, H., Hashimoto, K. and Kimura, I. 1980 Dependence of coherent nonlinear whistler interaction on wave amplitude. *J. Geophys. Res.* **85**, 644.

Neubert, T. and Banks, P. M. 1992 Recent results from studies of electron beam phenomena in space plasmas. *Planet. Space Sci.* **40**, 153.

Neubert, T., Taylor, W. W. L., Storey, L. R. O., Kawashima, N., Roberts, W. T., Reasoner, D. L., Banks, P. M., Gurnett, D. A., Williams, R. L. and Burch, J. L. 1986 Waves generated during electron beam emissions from the Space Shuttle. *J. Geophys. Res.* **91**, 11321.

Nishikawa, K. I., Frank, L. A. and Huang, C. Y. 1994 Three-dimensional simulation of whistler mode excited by the Spacelab 2 electron beam. *J. Geophys. Res.* **94**, 6855.

Omura, Y. and Matsumoto, H. 1982 Computer simulations of basic processes of coherent whistler wave–particles interactions in the magnetosphere. *J. Geophys. Res.* **87**, 4435.

O'Neil, T. M., Winfrey, J. H. and Malmberg, J. H. 1971 Nonlinear interaction of a small cold beam and a plasma. *Phys. Fluids* **14**, 1204.

Oraievsky, V., Chmyrev, V., Shibaev, I., Dokoukin, V., Sobolev, Ya., Shklyar, D. et al. 1994 Effects of artificially injected electron beams on the characteristics of ground VLF transmitter signals in the ionosphere. *J. Atmos. Terr. Phys.* **56**, 423.

Pivavorov, V., Burke, A., Ride, S. K. and Shapiro, V. D. 1995 Excitation of VLF waves by an electron beam injected into the ionosphere. *J. Geophys. Res.* **17**, 17515.

Porkolab, M. and Chang, R. P. H. 1978 Nonlinear wave effects in laboratory plasmas: comparison between theory and experiment. *Rev. Mod. Phys.* **50**, 745.

Raitt, W. J. 1996 Active plasma experiments in space: steps toward a space laboratory facility. In: *Review of Radio Science 1993–1996* (ed. by W. Ross Stone), p. 651. Oxford University Press.

Volokitin, A., Krafft, C. and Matthieussent, G. 1995 Whistler waves produced by a modulated electron beam: electromagnetic fields in the linear approach. *Phys. Plasmas* **2**, 4297.

Volokitin, A., Krafft, C. and Matthieussent, G. 1997 Whistler waves emission by a modulated electron beam: nonlinear theory. *Phys. Plasmas* **4**, 4126.

Winckler, J. R. 1980 The applications of artificial electron beams to magnetospheric research. *Rev. Geophys. Space Phys.* **18**, 659.

https://doi.org/10.1017/S0022377898007442 Published online by Cambridge University Press